Multinucleon Transfer Studies of the ^{70}Zn (15 MeV/nucleon) + ^{64}Ni System with Focus on Excitation Energy Distributions

Stergios Koulouris[1,*], *Georgios* Souliotis[1], *Francesco* Cappuzzello[2,3], *Diana* Carbone[3], *Athena* Pakou[4], *Cristina* Agodi[3], *Giuseppe* Brischetto[2,3], *Salvatore* Calabrese[3], *Manuela* Cavallaro[3], *Irene* Ciraldo[2,3], *Olga* Fasoula[1], *Onoufrios* Sgouros[3], *Vasileios* Soukeras[3], *Alessandro* Spatafora[2,3], *Domenico* Torresi[3], and *Martin* Veselsky[5]

[1]Laboratory of Physical Chemistry, Department of Chemistry, National and Kapodistrian University of Athens, Athens, Greece
[2]Dipartimento di Fisica e Astronomia "Ettore Majorana", Università di Catania, Italy
[3]Laboratori Nazionali del Sud, INFN, Catania, Italy
[4]Department of Physics and HINP, The University of Ioannina, Ioannina, Greece
[5]Institute of Experimental and Applied Physics, Czech Technical University, Prague, Czech Republic

Abstract. Existing high-resolution experimental data collected with the MAGNEX spectrometer were analyzed to investigate peripheral collisions of medium-mass nuclei from the reaction ^{70}Zn (15 MeV/nucleon) + ^{64}Ni. The main focus of this work was to correlate the observed ejectiles with the excitation energy of their progenitors. Experimental excitation energy distributions were generated and compared with the Deep-Inelastic Transfer (DIT) model. This revealed a dominance of direct reaction mechanisms located at low excitation energies and more complex mechanisms at higher energies. Future efforts include further detailed studies of the excitation energy distributions to elucidate the multinucleon transfer mechanisms and to comprehend the resolution limits achievable with medium-mass nuclei such as ^{70}Zn.

1 Introduction

The interest of the Nuclear Physics community in the study of nuclei away from the valley of beta stability has been kept vivid through the years [1–4]. Exploring the extremes of the nuclear landscape enables us to study various facets of the effective nuclear interaction, to understand various astrophysical processes, most notably the rapid neutron capture process (r-process), which plays a significant role in the production of half of the abundance of nuclides heavier than iron [5]. To advance further towards exotic neutron-rich nuclei, a fundamental approach is via multinucleon transfer and deep-inelastic reactions between heavy ions at low energies, namely near and above the Coulomb barrier. These reactions are mainly characterized by the sequential exchange of nucleons between the projectile-target binary system (e.g., [6]).

Motivated by observations from our group's recent contributions in the energy range of 15-25 MeV/nucleon [7–10], we proceeded to a project to produce projectile-like fragments with the use of the MAGNEX large-acceptance spectrometer at the INFN-LNS from the reaction of ^{70}Zn (15 MeV/nucleon) + ^{64}Ni. As presented in Ref.[11], we have developed a systematic procedure for the particle identification of the reaction products by reconstructing the atomic number Z of the ejectiles along with their ionic charge states employing measurements of the energy loss, residual energy and time-of-flight. Subsequently, we moved on to obtain the momentum and angular distributions of the ejectiles, as well as their isotopic production cross sections [12, 13]. In this contribution, we further extend our analysis by reconstruction of the excitation energy distributions of various reaction channels of the aforementioned reaction.

2 Experimental Apparatus and Data Reduction

The experiment was performed with the MAGNEX spectrometer [14, 15] at Istituto Nazionale di Fisica Nucleare, Laboratori Nazionali del Sud (INFN-LNS) in Catania, Italy. MAGNEX is a high-acceptance device which makes use of both the advantages of traditional magnetic spectrometry and those of a large angular and momentum acceptance detector. A ^{70}Zn^{15+} ion beam was delivered by the K800 Superconducting Cyclotron at the energy of 15 MeV/nucleon and impinged on a 1.18 mg/cm^2 ^{64}Ni target-foil. The optical axis of the spectrometer was set at an angle of θ_{opt} = 9° with respect to the beam axis, leading to a horizontal angular coverage of 4.0°-15.0°. In this experiment, the magnetic rigidity interval covered was in the range of 1.260-1.425 Tm. The ejectiles emerging from the target were detected by the MAGNEX focal plane detector (FPD) [16]. The FPD provides a simultaneous determination of the angles θ and ϕ of the ion's trajectory and the energy loss of the reaction products in the gas. Finally, the time-of-flight (TOF) of the ions was measured via a start signal from the silicon detectors of FPD and a stop signal

*e-mail: stekoul@chem.uoa.gr

from the radiofrequency of the cyclotron. In this experiment, for technical reasons, only a part of the FPD active area was used, further reduced due to optimization of the vertical angular acceptance, resulting finally to a solid angle acceptance of 5.4 msr.

By using the measured quantities provided by the FPD, the particle identification (PID) was carried out following the approach developed in Ref. [11] and applied in detail in Refs. [12, 13]. By setting graphical cuts in the Bρ versus E_{tot} plot, we obtained a two-dimensional distribution of the reaction angle (θ_{lab}) versus magnetic rigidity. Each channel in this plot, was stored and used as input for a data manipulation program developed in our laboratory. This program yields a four-dimensional distribution of the cross section with respect to Z, A, θ_{lab}, and momentum per nucleon (p/A), eventually resulting in momentum spectra, production cross sections, as well as excitation energy distributions of the ejectiles. We note that the momentum per nucleon (p/A) represents the velocity of the particles and can be a useful indicator of the energy dissipation caused by the interaction of the projectile with the target, offering crucial insights into the mechanism responsible for the production of the fragments of interest. The general behaviour of the momentum distributions that were fully analyzed in our work [12, 13] exhibit two primary regions: a) a quasielastic peak corresponding to direct processes, and b) a broad region at lower p/A values indicative of deep inelastic processes. In the following section, we will show results of reconstructed excitation energy distributions from various reaction channels. This comprises a parallel approach to that of the momentum distributions to further elucidate the reaction mechanism.

3 Results and Comparison with Theoretical Calculations

In this section, experimental results of ejectile distributions from the reaction of ^{70}Zn with ^{64}Ni at 15 MeV/nucleon will be described and compared with theoretical calculations. The calculations are based on a standard two-stage Monte Carlo approach. In the first, dynamical stage, the interaction between the projectile and the target was described by the phenomenological DIT model [17]. Following the dynamical stage of the reaction, the de-excitation of the primary fragments was described by the statistical de-excitation GEMINI code [18, 19]. For the purpose of this work, the combined calculations will be simply referred to as DIT calculations.

On panels (a)-(d) of Fig. 1, we present mass distributions for the observed isotopes of the elements with Z = 28–31 from the reaction ^{70}Zn (15 MeV/nucleon) with ^{64}Ni. The experimental data are shown by the closed black circles. The vertical dashed (green) line is an indicator for the starting point of neutron pickup. We note that the production of several neutron-rich nuclides corresponding to the pickup of 2–3 neutrons from the target has been achieved (e.g. in the case of Zn and Ga isotopes, respectively). In this figure also, the data are compared with the DIT calculations. We first focus our attention to the calculated yield distributions of the primary projectile-like fragments (quasiprojectiles) presented by the dotted (blue) lines. Their distributions are wide and nearly symmetric extending far to the neutron-rich side. The deexcitation of these excited primary products with the GEMINI code leads to the (cold) nuclides with cross sections depicted by the dashed (blue) lines. These distributions are more similar to the experimental data. While with solid (blue) lines we show the cross sections that have been appropriately filtered for the angular acceptance of MAGNEX and the magnetic rigidity interval of the experiment as mentioned in Sect. 2. We observe that the filtered DIT calculations lead to cross sections that are in overall reasonable agreement with the experimental data. The neutron-rich sides of the distributions are rather well described, with the exception of the Ga (Z=31) isotopes (one-proton pickup). Our current results may not lead to very neutron-rich nuclides as our research group's previous efforts using a 15 MeV/nucleon ^{86}Kr beam on ^{64}Ni and ^{124}Sn with the MARS separator [7]. The main reason of this result in the present experiment is due to limitations in the beam current imposed by the experimental setup, which accepted elastically scattered projectiles in the focal plane detector. With the ongoing upgrade of the MAGNEX facility [20] to accept higher rates, we are confident that this limitation will be surmounted, thus leading to the possibility of further experimental studies to produce very neutron-rich nuclides in the near future.

We continue with panels (e)-(h) of Fig. 1, where we present calculated mean excitation energy distributions of primary projectile fragments with the use of DIT. This plot represents a correlation of the mean excitation energies per nucleon of the primary (hot) fragments with the mass number of the de-excited final fragments. The primary fragments undergo subsequent de-excitation, resulting in the various nuclides shown in each frame of the figure. It is worth noticing that with an increase in the number of neutrons in the secondary products, the corresponding progenitors from which they originated had progressively lower excitation energies, reaching almost zero values in the very neutron-rich isotopes. This is a justified behaviour, as in order to detect such neutron-rich products, they must be quite 'cold', so that they can reach the detector without losing the captured neutrons. Concluding, the production of neutron rich products implies low excitation energies for the progenitors. In other words, the chance of surviving very neutron rich products has its origin to "cold" progenitors. And the challenge is: how can we obtain experimentally "cold" progenitors.

In panel (a) of Fig. 2, we present excitation energy distributions of ejectiles from the inelastic channel of the reaction ^{70}Zn (15 MeV/nucleon) + ^{64}Ni. We have attempted a preliminary reconstruction of the total excitation energy of the quasiprojectile (QP)-quasitarget (QT) binary system, that resulted in the observed fragments based on binary kinematics on an event-by-event basis. The procedure of reconstruction follows the approach reported in Ref.[22]. The reconstruction is performed under two different assumptions. The first assumption takes into account neutron emission only (closed black circles with full

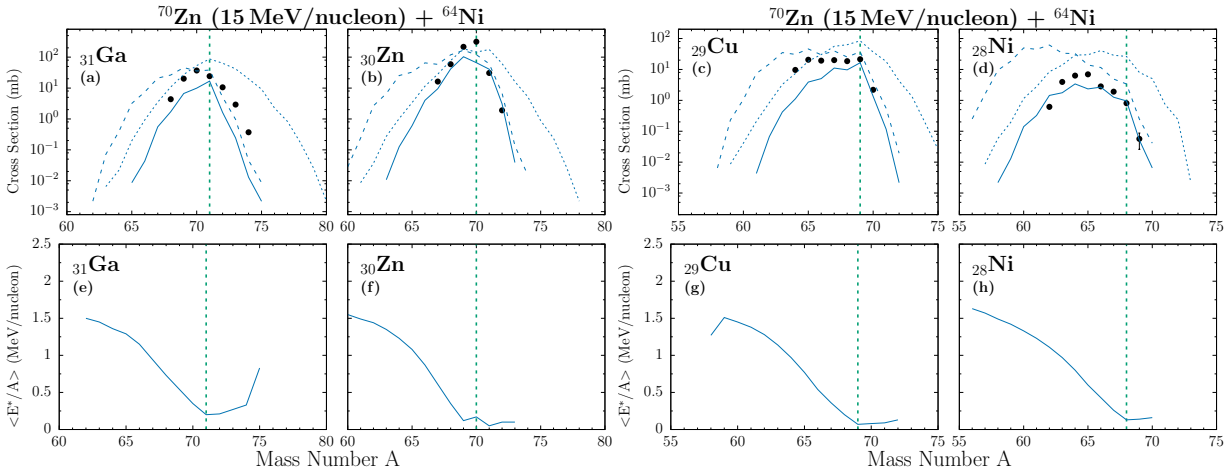

Figure 1. Panels (a)-(d): Production cross sections (mass distributions) of elements with Z=28-31 from the reaction ^{70}Zn (15 MeV/nucleon) + ^{64}Ni. Experimental Data: Closed (black) circles. DIT calculations are shown as follows: primary fragments with dotted (blue) line, final (cold) fragments with dashed (blue) line, and final fragments filtered for acceptance with the solid (blue) line. The vertical dashed (green) line indicates the initiation of neutron pickup. Panels (e)-(h): Calculated mean excitation energy per nucleon distributions of primary projectile fragments that lead to observed (cold) fragments of given mass number A.

lines). The second assumption represents the limit of no evaporation (black crosses with dashed lines). The obtained experimental data are compared with the DIT calculations shown by open (blue) circles. We have also extended our efforts to delve deeper into the reaction mechanism and the role of the primary fragments, by proceeding to a decomposition of the E* distributions of the ejectiles predicted by DIT. We make the assumption that the cold (final) fragments originate from primary quasiprojectiles that have picked up no neutrons (green squares), one neutron (purple diamonds), and two neutrons (yellow triangles), respectively, and lost subsequently via evaporation an equal number of neutrons. We will refer to these calculations as QP-λn, where λ = 0, 1, 2, meaning that the observed ejectile comes from a primary fragment (quasiprojectile, QP) which (after appropriate pickup) has evaporated no neutrons, one neutron, and two neutrons, respectively. The (orange) vertical dashed line at 20 MeV indicates an empirical threshold of quasielastic processes, defining the limit of no neutron emission from the QP. The vertical axis, presented as "diff. cross section," gives the value of $\frac{d^2\sigma}{dEd\Omega}$ in units of $[\frac{mb}{(MeV)msr}]$. We note that all the excitation energy distributions discussed in this work (as the p/A distributions of our previous work [12, 13]) are obtained in the polar angular range of θ_{lab} = 4 - 6° (and the azimuth range $\Delta\phi$ = 1.6°), thus corresponding to $\Delta\Omega$ = 1.0 msr. We have checked that if the distributions are obtained in the full angular range θ_{lab} = 4 - 15°, the shape of the distributions does not change whereas the cross sections are slightly increased. The general behaviour of the reconstructed excitation energy distributions is a progressive decrease of the cross section with respect to the increase of the total excitation energy of the primary binary system. The experimental distributions are compared with the components of the DIT calculation, with the following qualitative correspondence: the QP-0n calculation is in good agreement with the behaviour of the data in the quasielastic region (low excitation energy), the QP-1n calculation describes the middle area of the distribution, while the QP-2n calculation describes the tails of the excitation energy distributions in the dissipative region (high total excitation energy). The following observations are in line: the experimental data obtained under the assumption of no evaporation extend to larger excitation energies compared to the data obtained assuming neutron evaporation only. Moreover, the experimental data are higher than the calculations, possibly implying the existence of inelastic excitation mechanisms that cannot be described by the DIT model. We note that this behaviour is in agreement with the conclusions obtained from our previous study of the p/A distributions [12].

In panel (b) of Fig. 2, we present the DIT calculated correlation of the mean excitation energy of primary quasiprojectiles leading to ^{70}Zn as a function of the total excitation energy of the QP-QT system. The open (blue) circles are from the full DIT calculation and show that the QP obtains nearly half of the available total excitation energy, as expected from peripheral collisions involving nucleon exchange (see [22] and references therein). The open (green) squares indicate the QP-0n component of the DIT calculation indicating the limit of no neutron emission. Furthermore, the open (purple) diamonds and the open (yellow) triangles present the QP-1n and QP-2n component of the DIT calculations. These correlations are rather flat indicating the corresponding thresholds for 0n, 1n and 2n emission from the QP to give the ^{70}Zn ejectile.

In a fashion similar to Fig. 2(a), we present in Fig. 3 the reconstructed excitation energy distributions of ejectiles from one- and two- neutron pickup channels [panels (a)-(b)] and the single charge exchange channel [panel (c)].

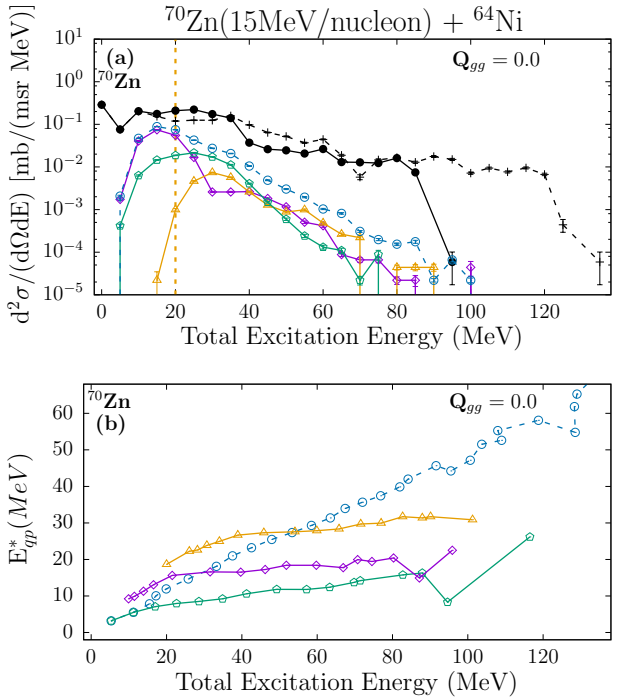

Figure 2. Panel (a): Reconstructed excitation energy distributions of ejectiles from the inelastic channel of the reaction ^{70}Zn (15 MeV/nucleon) + ^{64}Ni. Experimental Data: Neutron evaporation-only [closed (black) circles with full lines], no evaporation limit [(black) crosses with dashed lines]. Panel (b): Calculated excitation energy of primary quasiprojectiles leading to ^{70}Zn as a function of the total excitation energy of the primary quasiprojectile - quasitarget system. The DIT calculation is shown with open (blue) circles. Three further components of the DIT decomposition, QP-0n, QP-1n and QP-2n, are shown under the assumption that the primary fragment (the quasiprojectile, QP) undergoes pick up of no neutrons [open (green) squares], one neutron [open (purple) diamonds] and, two neutrons [open (yellow) triangles] and subsequent evaporation of them (see text).

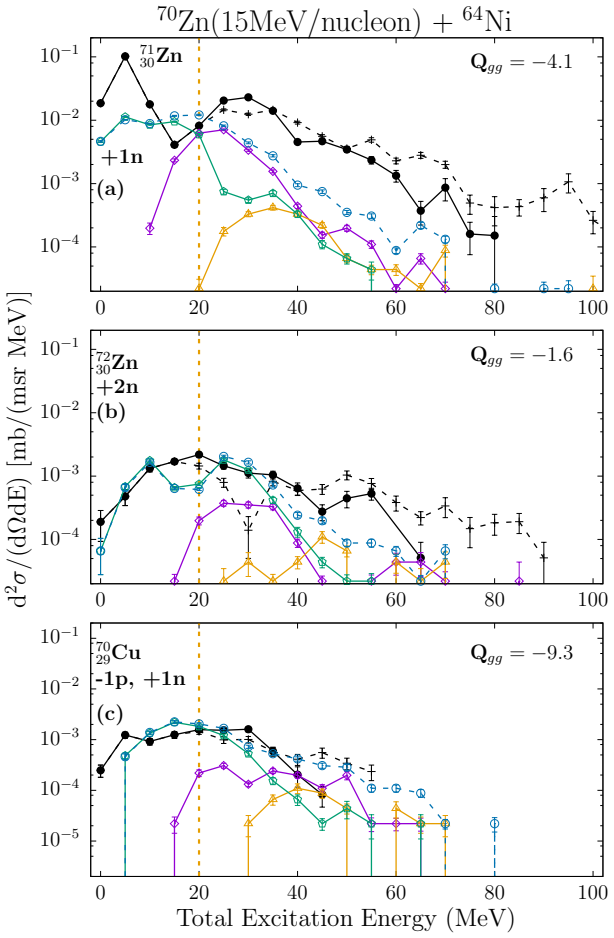

Figure 3. Reconstructed excitation energy distributions of ejectiles from nucleon pickup channels of the reaction ^{70}Zn (15 MeV/nucleon) + ^{64}Ni. Experimental Data: Neutron evaporation-only [closed (black) circles with full lines], no evaporation limit [(black) crosses with dashed lines]. The DIT calculation is shown with open (blue) circles. Three further components of the DIT decomposition, QP-0n, QP-1n and QP-2n, are shown under the assumption that the primary fragment (the quasiprojectile, QP) undergoes pick up of no neutrons [open (green) squares], one neutron [open (purple) diamonds] and, two neutrons [open (yellow) triangles] and subsequent evaporation of them.

Interestingly, in Fig. 3(a) we observe a pronounced experimental peak at low excitation energy that corresponds to direct 1n pickup. We note that it cannot be described by the QP-0n calculation, as DIT describes only a stochastic exchange of nucleons. Also the data above 20 MeV are, as in the case of the inelastic channel, higher than the DIT calculation, hinting again at mechanisms of inelastic excitation followed by transfer that cannot, of course, be described by DIT. The (+2n) and (-1p+1n) channels appear to be described well by the DIT calculations.

Finally in Fig. 4 we present the excitation energy distributions of nucleon stripping channels. Conclusions similar to Fig. 3 may be drawn. Specifically, in the (-1n) and (-2n) channels, the data are above the DIT calculations, possibly pointing at mechanisms beyond nucleon exchange. The QP-0n component of DIT roughly describes the regions below 20 MeV, whereas above 20 MeV the other two components QP-1n, QP-2n progressively take part (but as already mentioned, the calculations are lower than the data).

4 Conclusions

This work represents part of our detailed investigations of peripheral reactions of medium-mass nuclei in the Fermi energy regime based on experimental measurements of ejectiles from the reaction ^{70}Zn + ^{64}Ni at 15 MeV/nucleon studied with the MAGNEX spectrometer. The MAGNEX facility enabled us to obtain high-resolution measurements of the momentum and the reaction angle of medium mass ejectiles in an extended region from quasielastic to deep-inelastic processes. Specifically, in this work we attempted

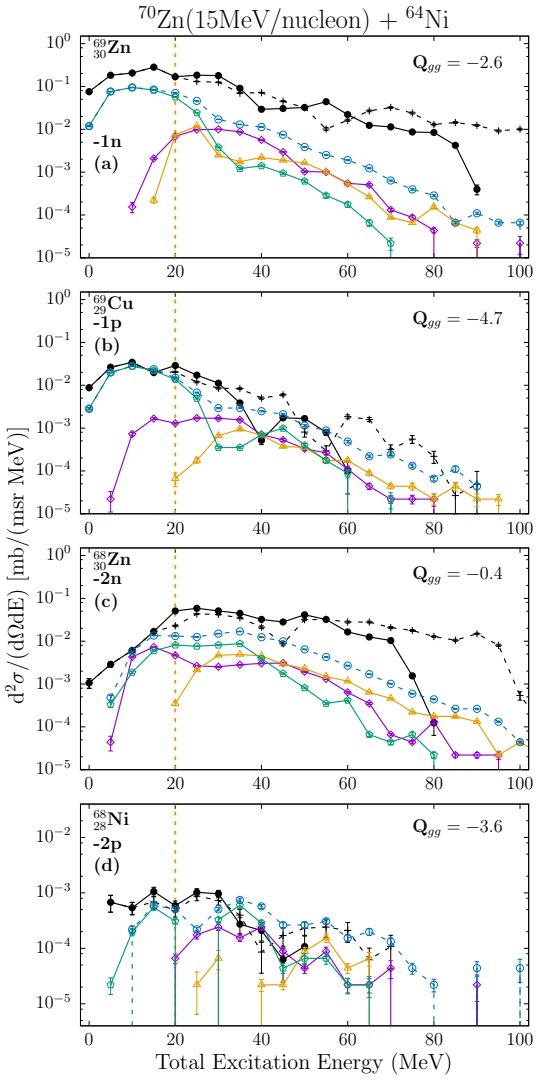

Figure 4. Reconstructed excitation energy distributions of ejectiles from stripping channels of the reaction ^{70}Zn (15 MeV/nucleon) + ^{64}Ni. Experimental Data: Neutron evaporation-only [closed (black) circles with full lines], no evaporation limit [(black) crosses with dashed lines]. The DIT calculation is shown with open (blue) circles. Three further components of the DIT decomposition, QP-0n, QP-1n and QP-2n, are shown under the assumption that the primary fragment (the quasiprojectile, QP) undergoes pick up of no neutrons [open (green) squares], one neutron [open (purple) diamonds] and, two neutrons [open (yellow) triangles] and subsequent evaporation of them.

to correlate the observed ejectiles with the excitation energy of their progenitors in binary collisions through kinematical reconstruction and DIT calculations.

The detailed study of ejectiles under this new perspective indicated clearly, similar to comparisons as a function of p/A (see Ref.[12, 13]), the dominance of direct reaction mechanisms at low excitation energy (below about 20 MeV) and the appearance of more complicated processes (even beyond independent nucleon exchange) at higher excitation energy. Moreover it was found that the chance of surviving of very neutron-rich products has its origin in "cold" progenitors, and that the quasiprojectile (i.e. the progenitor of the ejectile) carries on average about 1/2 of the total excitation energy. These findings give us the initiative for new future work, including detailed studies of the excitation energy correlation and sharing between the participants of a binary collision and the conditions under which one of them may remain relatively "cold", thus minimizing (or avoiding) neutron evaporation.

Finally, our plans include efforts to reconstruct the excitation energy with the maximum possible resolution attainable in our analysis in order to examine the possibility to perform charged particle spectroscopy.

5 Acknowledgements

We are grateful to the support staff of INFN–LNS for providing the primary beam. This project has received funding from the European Research Council (ERC) under the European Unions Horizon 2020 research and innovation programme (grant agreement No 714625). GS and SK acknowledge support from the Special Account for Research Grants of the National and Kapodistrian University of Athens. MV was supported by the Czech Science Foundation (GACR) grant No. 21-24281S.

References

[1] T. Mijatovic, Multinucleon transfer reactions: a mini-review of recent advances. Front. Phys. **10**, 965198 (2022). https://doi.org/10.3389/fphy.2022.965198

[2] G. G. Adamian, N. V. Antonenko, A. Diaz-Torees, and S. Heinz, How to extend the chart of nuclides?. Eur. Phys. J. A **56**, 47 (2020). https://doi.org/10.1140/epja/s10050-020-00046-7

[3] F. Nowacki, A. Obertelli, and A. Poves, The neutron-rich edge of the nuclear landscape: Experiment and theory. Prog. Part. Nucl. Phys. **120**, 103866 (2021). https://doi.org/10.1016/j.ppnp.2021.103866

[4] L. Corradi, G. Pollarolo, and S. Szilner, Multinucleon transfer processes in heavy-ion reactions. J. Phys. G: Nucl. Part. Phys. **36**, 113101 (2009). https://doi.org/10.1088/0954-3899/36/11/113101

[5] J. J. Cowan, C. Sneden, J. E. Lawler, A. Aprahamian, M. Wiescher, K. Langanke, G. Martinez-Pinedo, and F. K. Thielemann, Origin of the heaviest elements: The rapid neutron-capture process. Rev. Mod. Phys. **93**, 015002 (2021). https://doi.org/10.1103/RevModPhys.93.015002

[6] T. Mijatovic, S. Szilner, L. Corradi, D. Montanari, G. Pollarolo, E. Fioretto et al., Multinucleon transfer reactions in the ^{40}Ar + ^{208}Pb system. Phys. Rev. C **94**, 064616 (2016). https://doi.org/10.1103/PhysRevC.94.064616

[7] G. A. Souliotis, M. Veselsky, S. Galanopoulos, M. Jandel, Z. Kohley, L. W. May, D. V. Shetty, B. C. Stein, and S. J. Yennello, Approaching neutron-rich nuclei toward the r-process path in peripheral heavy-ion collisions at 15 MeV/nucleon. Phys. Rev. C **84**, 064607 (2011). https://doi.org/10.1103/PhysRevC.84.064607

[8] A. Papageorgiou, G. A. Souliotis, K. Tshoo, S. C. Jeong, B. H. Kang, Y. K. Kwon, M. Veselsky, S. J. Yennello, and A. Bonasera, Neutron-rich rare isotope production with stable and radioactive beams in the mass range A ∼ 40–60 at beam energy around 15 MeV/nucleon. J. Phys. G **45**, 095105 (2018). https://doi.org/10.1088/1361-6471/aad7df

[9] O. Fasoula. G. A. Souliotis, S. Koulouris, K. Palli, M. Veselsky, S. Yennello, and A. Bonasera, Study of multinucleon transfer mechanisms in ^{86}Kr-induced peripheral reactions at 15 and 25 MeV/nucleon. HNPS Adv. Nucl. Phys. **28**, 47 (2022). https://doi.org/10.12681/hnps.3572

[10] K. Palli, G. A. Souliotis, I. Dimitropoulos, T. Depastas, O. Fasoula, S. Koulouris, M. Veselsky, S. J. Yennello, and A. Bonasera, Microscopic description of multinucleon transfer in ^{40}Ar + ^{64}Ni collisions at 15 MeV/nucleon. EPJ Web Conf. **252**, 07002 (2021). https://doi.org/10.1051/epjconf/202125207002

[11] G. A. Souliotis, S. Koulouris, F. Cappuzzello, D. Carbone, A. Pakou, C. Agodi et al., Identification of medium mass (A=60-80) ejectiles from 15 MeV/nucleon peripheral heavy-ion collisions with the MAGNEX large-acceptance spectrometer. Nucl. Instrum. Methods A **1031**, 166588 (2022). https://doi.org/10.1016/j.nima.2022.166588

[12] S. Koulouris, G. A. Souliotis, F. Cappuzzello, D. Carbone, A. Pakou, C. Agodi et al., Multinucleon transfer channels from ^{70}Zn (15 MeV/nucleon) + ^{64}Ni collisions. Phys. Rev. C **108**, 044612 (2023). https://doi.org/10.1103/PhysRevC.108.044612

[13] S. Koulouris, G. A. Souliotis, F. Cappuzzello, D. Carbone, A. Pakou, C. Agodi et al., Measurements of projectile fragments from ^{70}Zn + ^{64}Ni collisions with the MAGNEX spectrometer at INFN-LNS. HNPS Adv. Nucl. Phys. **28**, 42 (2022). https://doi.org/10.12681/hnps.3571

[14] F. Cappuzzello, C. Agodi, D. Carbone, M. Cavallaro, The MAGNEX spectrometer: Results and perspectives. Eur. Phys. J. A **52**, 167 (2016). https://doi.org/10.1140/epja/i2016-16167-1

[15] M. Cavallaro, C. Agodi, G. A. Brischetto, S. Calabrese, F.Cappuzzello, D. Carbone et al., The MAGNEX magnetic spectrometer for double charge exchange reactions. Nucl. Instrum. Methods B **463**, 334 (2020). https://doi.org/10.1016/j.nimb.2019.04.069

[16] D. Torresi, O. Sgouros, V. Soukeras, M. Cavallaro, F. Cappuzzello, D. Carbone et al., An upgraded focal plane detector for the MAGNEX spectrometer, Nucl. Instrum. Methods A **989**, 164918 (2021). https://doi.org/10.1016/j.nima.2020.164918

[17] L. Tassan-Got and C. Stephan, Deep inelastic transfers: a way to dissipate energy and angular momentum for reactions in the Fermi energy domain. Nucl. Phys. A **524**, 121 (1991). https://doi.org/10.1016/0375-9474(91)90019-3

[18] R. J. Charity, M. A. McMahan, G. J. Wozniak, R. J. McDonald, L. G. Moretto, D. G. Sarantites et al., Systematics of complex fragment emission in niobium-induced reactions. Nucl. Phys. A **483**, 371 (1988). https://doi.org/10.1016/0375-9474(88)90542-8

[19] R. J. Charity, N-Z distributions of secondary fragments and the evaporation attractor line, Phys. Rev. C **58**, 1073 (1998). https://doi.org/10.1103/PhysRevC.58.1073

[20] C. Agodi, A. D. Russo, L. Calabretta, G. D'Agostino, F. Cappuzzello, M. Cavallaro et al., The NUMEN project: Toward new experiments with high-intensity beams. Universe **7**, 72 (2021). https://doi.org/10.3390/universe7030072

[21] H. Lenske, F. Cappuzzello, M. Cavallaro, and M. Colonna, Heavy ion charge exchange reactions as probes for nuclear β-decay. Prog. Part. Nucl. Phys. **109**, 103716 (2019). https://doi.org/10.1016/j.ppnp.2019.103716

[22] G. A. Souliotis, P. N. Fountas, M. Veselsky, S. Galanopoulos, Z. Kohley, A. McIntosh, S. J. Yennello, and A. Bonasera, Isoscaling of heavy projectile residues and N/Z equilibration in peripheral heavy-ion collisions below the Fermi energy. Phys. Rev. C **90**, 064612 (2014). https://doi.org/10.1103/PhysRevC.90.064612